J. KAU: Met., Env., Arid Land Agric. Sci., **Vol. 6**, pp. 57-71 (1415 A.H. / 1995 A.D.)

Estimation of Surface Soil Moisture in a Semi-Arid, Mountainous Region Using Satellite Microwave Observations: A Case Study of Southwestern Region of Saudi Arabia

ABDUL-WAHAB S. MASHAT
Faculty of Meteorology, Environment and Arid Land Agriculture, King Abdulaziz University, Jeddah, Saudi Arabia

ABSTRACT. This study presents the use of passive microwaves to classify and estimate the surface soil moisture in a semi-arid, mountainous region. The southwestern region of Saudi Arabia was chosen for this study. Two case studies have been considered to investigate the response of Special Sensor Microwave/Imager (SSM/I) brightness temperature to soil moisture. The first case is at satellite ascending overpass time (about 6:00 a.m. local solar time), and the second one is at satellite descending overpass time (about 6:00 p.m. local solar time). It is shown that normalized brightness temperature with respect to ground temperature may be interpreted in terms of the soil moisture in the surface layers. Normalized brightness temperature is not sensitive to soil moisture when precipitating clouds are present. The existence of precipitating clouds over the study area was determined through examination of the brightness temperature of frequency 85.5 GHz (Gigahertz).

Introduction

Soil moisture information over large areas is an important physical variable for meteorological, hydrological and agricultural applications. In meteorology, information about soil moisture is needed for providing a boundary condition variable for dynamic atmospheric models. In hydrology and agriculture, information about soil moisture can be used in flood forecasting, crop yield forecasting, and irrigation scheduling. Thus, accurate estimation of soil moisture for large areas are helpful when obtained within short time periods. However, direct measurement of soil moisture over large areas is difficult because of the cost of installation and operation of the needed instruments. Remote sensing methods, therefore, which are based on

change in the electromagnetic properties of soil when water is added, provide a way to determine the spatial distribution of soil moisture over large areas within short time periods.

Previous studies (Schmugge *et al.* 1979; Schmugge 1983) have been limited to flat terrain with reasonably uniform vegetation but, even with these restrictions, the most successful results have led only to classification or categorization of soil moisture amount. This research is an attempt to move into a more challenging topographical environment such as a semi-arid, mountainous region in which vegetation varies from lush to bare land. In mountain regions, variations in vegetation density, soil type, precipitation amount, ground temperature, and topographic characteristics are large within small areas. For this reason, it is more difficult to determine soil moisture distribution over mountain regions than over flat, bare surfaces or uniform agricultural areas.

Encouraging progress has occurred with the launching of the Special Sensor Microwave/Imager (SSM/I) with its seven channels improving scanning capabilities and gaining better resolution. With the advent of the SSM/I, opportunities now exist to improve estimate or classification of soil moisture over mountainous regions if the effects of surface heterogeneity can be eliminated or reduced.

The objective of this research is to use the observed microwave brightness temperatures from the SSM/I to obtain estimate of soil moisture in near-surface layers for the southwestern region of Saudi Arabia.

Background

During the last two decades, progress has been made in studying the relationship between near-surface soil moisture content and brightness temperature as measured by microwave radiometers. Theoretical (*e.g.*, Njoku and Kong 1977; Wilheit 1978; Burke *et al.* 1979) and experimental (*e.g.*, Newton 1977; Schmugge 1978; Newton and Rouse 1980; Njoku and O'Neill 1982) studies have shown a strong correlation between soil moisture content and brightness temperature measured remotely by using passive microwave sensors. Previous research results (Schmugge *et al.* 1979; Schmugge 1983) have shown that passive microwave remote sensing can be used to classify near-surface soil moisture.

Poe and Edgerton (1971) investigated the relationship between the moisture content of a bare soil and its emissivity. They found that the emissivity of a smooth, bare area varies from 0.9 or greater for dry soil to about 0.5 for wet soil. Their results were based on microwave radiometric measurements at wavelengths of 0.81, 2.2, 6.0, and 21.4 cm. Schmugge *et al.* (1974) reported that microwave radiometers are sensitive for monitoring soil moisture content over depths on the order of a few centimeters. The emission is a function of soil moisture and radiometer frequency. They found that, in aircraft tests at frequency of 19.35 GHz (Gigahertz) little or no variation is present in soil emission if its moisture is less than 15% water content by weight. However, when its moisture is between 15% and 40% water content, the emission de-

creases linearly by approximately 3°K (Kelvin) for each percentage point. In contrast, the emission at 21 cm (1.4 GHz) is a linear function of soil moisture content over the 0-35% moisture range. Burke and Paris (1975) used measured brightness temperatures at vertical (*Tv*) and horizontal (*Th*) polarizations to estimate moisture of the top centimeter of soil. They showed that the Stokes parameters [*Tv* + *Th*]/2 and [*Tv-Th*] can be used to distinguish between moisture and surface roughness effects. Eagleman and Lin (1976) compared the observed brightness temperatures from Skylab over Texas, Oklahoma, and Kansas with soil moisture based on a combination of actual ground measurements and estimated soil moisture using a climatic water balance model. They found a strong correlation (– 0.96) between the 21 cm (1.4 GHz) brightness temperature and the estimated soil moisture of the upper 2.5-cm soil layer.

The antecedent precipitation index (API), which is a soil moisture model that requires only the precipitation amount as input, has been used to indicate soil moisture conditions and correlate it with microwave brightness temperature. Assuming that reflectivity from clouds is negligible and that atmospheric transmissivity is 1.0, McFarland (1976) has shown a relationship between the Skylab 21-cm (1.4 GHz) brightness temperature for data obtained over Texas and Oklahoma and API. Using the same assumptions and the passive microwave data, McFarland and Blanchard (1977), Blanchard *et al.* (1981), McFarland and Harder (1982), Wilke (1984), and Wilke and McFarland (1986) presented strong correlations between API and the normalized brightness temperature.

The Study Area

The area of study, southwestern region of Saudi Arabia, is bounded by Yemen in south; latitude 20°N in north, longitude 43°30′E in east, and Red Sea in west. Because of the spatial resolution of the satellite, the study area was divided into small grid cells with dimensions 0.25° × 0.25°. Grid cells that are at least 0.25° from the sea and have at least one rainfall station with continuous daily rainfall data during the period July 1st through August 30th, 1987 were considered in this study. Thirty-three grid cells in the study area have met the above conditions (Table 1). The cells were numbered from the northwest beginning with number 1 and ending with number 33 (Fig. 1).

TABLE 1. Average elevation (above sea level) and number of rainfall stations in each grid cell.

Grid cell	Average elevation above sea level (m)	Number of rainfall stations
1	2300.0	2
2	2100.0	2
3	1500.0	4
4	1200.0	2

TABLE 1. Contd.

Grid cell	Average elevation above sea level (m)	Number of rainfall stations
5	1200.0	1
6	1600.0	3
7	800.0	1
8	1200.0	8
9	2400.0	2
10	2000.0	1
11	600.0	3
12	800.0	4
13	2200.0	7
14	1700.0	2
15	1800.0	1
16	1400.0	3
17	2400.0	2
18	2100.0	2
19	2000.0	1
20	1000.0	1
21	2300.0	4
22	2100.0	4
23	2000.0	2
24	1600.0	1
25	2000.0	2
26	2300.0	2
27	1200.0	2
28	1300.0	3
29	300.0	3
30	800.0	2
31	200.0	3
32	600.0	6
33	100.0	4

Data Collection and Preparation

The data used in this investigation contained passive microwave data from the Special Sensor Microwave/Imager (SSM/I) for the southwestern region of Saudi Arabia for the period from 01 July to 30 September, 1987. Meteorological data used were extracted from the records of the Meteorology and Environmental Protection Administration (MEPA), Ministry of Defence and Aviation, Kingdom of Saudi Arabia, and the Hydrology Division, Ministry of Agriculture and Water, Kingdom of Saudi Arabia.

Satellite Data

The SSM/I is a passive multichannel microwave radiometer deployed on the Defense Meteorological Satellite Program (DMSP) Block 5D-2 F8 satellite, which was

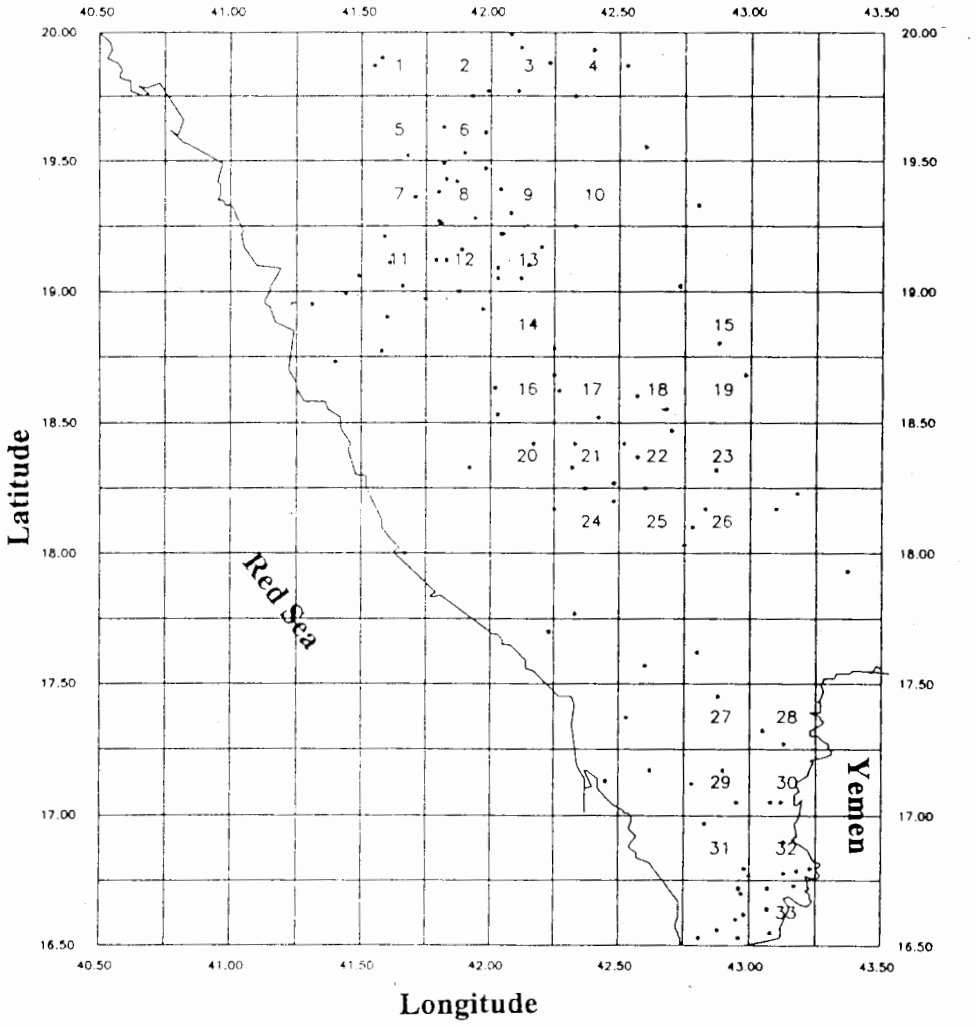

FIG. 1. Location of the used rainfall stations in the southwestern region of Saudi Arabia.

launched into a near-polar orbit in June, 1987. The satellite is at an altitude of about 833 km with an orbit period of 102 min. The orbit produces 14 revolutions a day.

The SSM/I scans the Earth in a conical pattern with a swath width of 1400 km and an earth-incidence angle of 53.1°. It measures upwelling radiation at values of frequency 19.35, 37.0 and 85.5 GHz for both vertical and horizontal polarization, and frequency 22.235 GHz for only vertical polarization. SSM/I covers the globe twice a day, so it is possible to get two passes over Saudi Arabia per day at about 6 a.m. local solar time (Node A) and 6 p.m. local solar time (Node D). Only a limited amount of

data were available, as shown in Table 2, which presents a list of the satellite data used in this research.

TABLE 2. Available overpass SSM/I data for southwestern region of Saudi Arabia at Nodes A and D during the period July 1st through September 30th, 1987.

Overpass calendar date (1987)	
Node A	Node D
193	192
199	206
206	215
224	216
225	224
231	225
232	226
233	232
234	233
247	234
248	235
249	242
250	249
256	250
259	251
267	257
272	258
273	265
	274

Ground Truth Data

Soil moisture at any point is affected by a number of factors such as amount of initial soil moisture, precipitation, surface runoff, and actual evapotranspiration (*AET*). Therefore, to estimate soil moisture, which will be considered as "ground truth," the daily precipitation amounts measured by rain gages, and the daily *AET* are needed.

AET will be estimated from potential evapotranspiration (*PET*), which was calculated by Linacre method (Linacre, 1977). The value of *AET* differs from the value for *PET* under most environments since *AET* depends on the amount of available water and plant characteristics such as root depth. *AET* is less than *PET,* whereas *PET* is approximately equal to the evaporation from a large free-water surface, such as a lake. The relation between *AET* and *PET* has been the subject of much discussion in the literature (Griffiths 1982). Most of researchers agree that the value of *AET* is about the same as the value of *PET* when adequate moisture is available and tends to zero when moisture is low. However, between these boundaries they have different opinions about the ratio between *AET* and *PET*. In this research, the relation between *AET* and *PET* is adopted as *AET* equals *PET* when the soil moisture

on the previous day is greater than zero, and AET equals zero when the soil moisture on the previous day is zero.

The temporal and spatial patterns of soil moisture, using precipitation and estimated AET data, are needed as "ground truth" value of soil moisture on day of study i (SM_i) over the entire study period at a given grid cell was computed, in millimeters, using the following model :

$$SM_i = SM_{i-1} + P - (AET + R), \tag{1}$$

where SM_{i-1} is the soil moisture on the previous day, P is the precipitation amount, AET is the actual evapotranspiration, and R is the runoff outflow. In the region and during the period of study, the runoff outflow R is small and can be neglected. Therefore, Eq. (1), with a lower limit for SM_i is equal to zero, can be written as

$$SM_i = SM_{i-1} + P - AET. \tag{2}$$

The value of soil moisture at about 6:00 a.m. and 6:00 p.m. local solar time is needed to compare it with the SSM/I data. Often in summer, rain occurs in the afternoon. The equation used to calculate soil moisture at satellite descending overpass time (Node D, about 6:00 p.m. local solar time) is

$$SM_i = (SM_{i-1} - AET) + P, \tag{3}$$

with the minimum value inside the parenthesis equal to zero. On the other hand, with assumption that AET is small at night and can be neglected, the equation used to calculate soil moisture at the satellite ascending overpass time (Node A, about 6:00 a.m. local solar time) is

$$SM_i = SM_{i-1} . \tag{4}$$

The initial value for SMi for each grid cell is selected to be zero after five dry days.

Ground Temperature

Because of the topographical difference in each grid cell, elevation correction for temperature is needed. The regression analysis of monthly mean temperature and station's elevation for the available stations (twelve stations) for each month (July-September, 1987) shows large values of the square of the linear correlation coefficient, R^2. For maximum temperatures, the coastal station (Gizan) has been excluded. When Gizan data are included, values of R^2 is lower in value (0.78 for July, 0.82 for August, and 0.88 for September) are lower than values when excluding them (0.94 for July, and 0.97 for August and September). This is caused by the sea breeze during the day. For minimum temperature values, all the stations have been used in the regression analysis giving R^2 to be 0.72, 0.89, and 0.73 for July, August, and September, respectively.

The average elevation for each grid cell (Table 1) has been approximated using the maps of the study area prepared by the United States Geological Survey for the Kingdom of Saudi Arabia using computer-enhanced LANDSAT MSS Band 7 imagery. Daily maximum and minimum temperature for each grid cell were estimated

from the daily fluctuations of temperature from the mean value for each station located close to the cell. The estimated minimum temperature for each grid cell is assumed to represent the ground temperature at satellite ascending overpass time (about 6:00 a.m. local time), whereas the estimated mean temperature for each grid cell ($T_{max} + T_{min}$) / 2 is assumed to represent the ground temperature at satellite descending overpass time (about 6:00 p.m. local time).

Analysis and Discussion

All Data

The initial analysis consisted of two data sets of all the 33 grid cells. The first data set (467 observations) is for the satellite ascending overpass time (Node A, about 6:00 a.m. local solar time), and the second data set (550 observations) is for the satellite descending overpass time (Node D, about 6:00 p.m. local solar time). Each data set contains the grid cell number; Julian date; brightness temperature values ($V19$, $H19$, $V22$, $V37$, $H37$, $V85$, and $H85$, where V is vertical polarization, H is horizontal polarization, and 19, 22, 37, and 85 are frequencies 19.350, 22.235, 37.00, and 85.5000 GHz, respectively), ground temperature (T); normalized brightness temperatures (or emissivities, which are defined at each frequency for each grid cell as T_b/T where T_b is the brightness temperature at given SSM/I frequency); and values of calculated soil moisture SM. Statistical regression analyses for all available data for Nodes A and D were performed.

Low correlation coefficients ($R^2 = 0.14$) occur between the SSM/I brightness temperatures or the normalized brightness temperatures and soil moistures SM. This is a result of differences in emissivity among the grid cells. For examples, the average emissivity or normalized brightness temperature ($V19/T$) for Channel $V19$, Node D for each grid cell for dry-land, is illustrated in Fig. 2. It shows that emissivity ($V19/T$) varies considerably from grid cell to grid cell with a maximum of 0.9721, a minimum of 0.9396, a mean of 0.9561, and standard deviation of 0.0092. It is found that grid cells sited in the peak or east side of the mountains have greater emissivity than grid cells located in the west side. The exception is for grid cells that are partially covered by vegetation, such as Grid Cells 26 and 23. Each grid cell was studied individually to eliminate features that differ among the cells, such as topography, vegetation cover, soil type, climate, etc.

Correction for Precipitating Clouds

The presence of precipitating clouds will influence values of brightness temperature. Therefore, data with precipitating clouds should be excluded from the analysis. Unfortunately, hourly rainfall information is not available for this research, so daily rainfall had to be used. Ideally, a method is needed to identify the existence of precipitating clouds at the time of the satellite overpass. The existence of precipitating clouds will mask the radiation emitted from the ground surface, and the scattering effect of rain and cloud droplets increases with increasing frequency.

For SSM/I frequencies, the $V85$ and $H85$ channels are more strongly attenuated by precipitating clouds, but the $V19$ and $H19$ channels are least affected by the presence

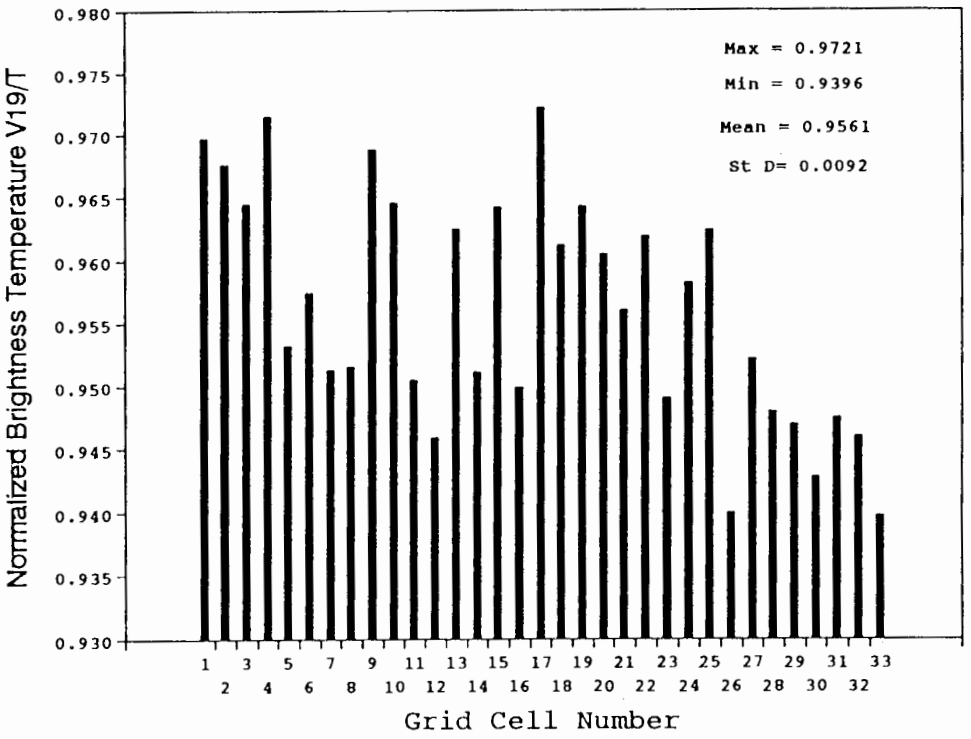

FIG. 2. Average normalized brightness temperature ($V19/T$) for each grid cell (dry soil) at node D(N values vary between 6 and 17).

of precipitating clouds. The $H85$ channel measurements will be scattered by hydrometeors in the atmosphere in a similar manner as the $V85$ channel. The existence of precipitating clouds over the study area can likely be determined through an examination of the channels $V85$ and $H19$. The lower brightness temperature of the $V85$ channel may indicate the presence of precipitating clouds. This is because channel $V85$ is strongly attenuated by precipitating clouds. Therefore, the existence of precipitating clouds would be examined only by using SSM/I brightness temperatures such that when $H19 - V85 > 0$. For Node A, it was found that all the data had $H19 - V85 < 0$, and they will be used in the analysis. However, for Node D several data points were excluded because of having $H19 - V85 > 0$. These agree with the synoptic situation over southwestern part of Saudi Arabia at this time of year where clouds form and rainfall occurs in the afternoon over the region.

Case Studies

To investigate the response of the normalized brightness temperatures of SSM/I to soil moisture, two case studies were conducted. The first case study is Node A at Grid Cell 16 and the second one is Node D at Grid Cell 12. These two grid cells were selected to provide better "ground truth" data for their having high range of soil

moisture (20 mm), providing several SSM/I observations immediately after rainfall, and including several rainfall stations (three rainfall stations in each grid cell).

For each grid cell, a time series chart was developed for the entire period of the available SSM/I data from 1 July to 10 September, 1987 (days 182-273 on the Julian calendar). Figures 3 and 4 show the responses of the normalized brightness temperatures to the soil moisture caused by rainfall in Grid Cells 16 and 12 for Nodes A and D, respectively. For all frequencies, values of the normalized brightness temperature were reduced after rainfall; and then increased when it becomes dry.

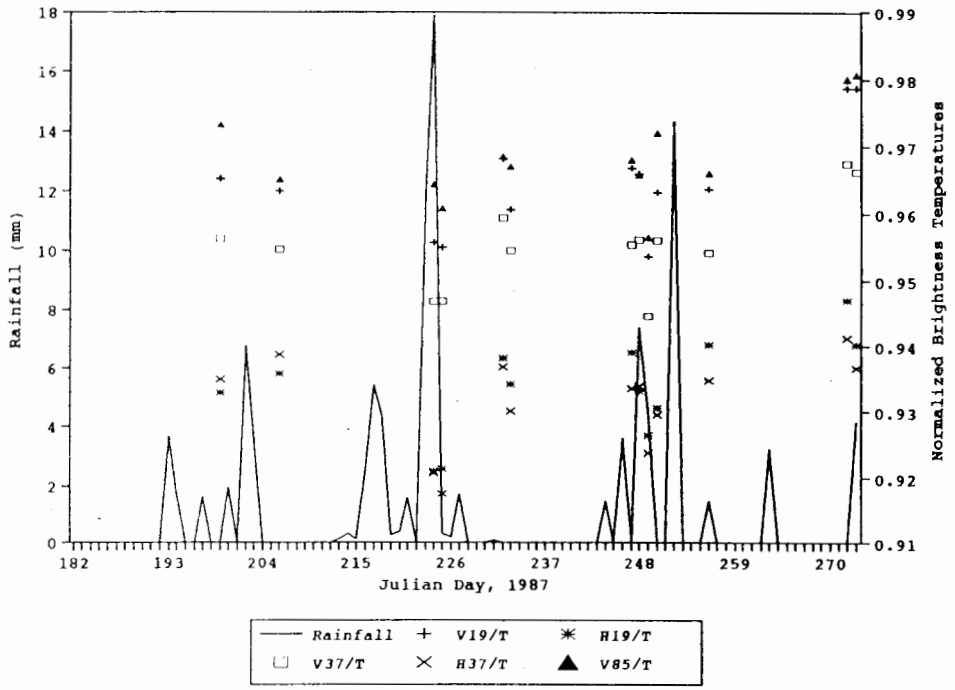

FIG. 3. Time series plots of rainfall and the normalized brightness temperatures for Grid Cell 16 (Node A) between 1 July and 30 September, 1987.

The quantitative temporal analysis involved correlating the computed soil moisture *SM* with the SSM/I brightness temperature of the seven channels and the various transformation values of the SSM/I brightness temperature. All the available data as well as the filtered one excluding the precipitating clouds (*i.e.*, when $H19 - V85 < 0$) were used. The various values of transformation of the brightness temperature include the normalized brightness temperature with respect to the ground temperature, the ratio or difference between any two of the seven channels, and the polarization ratio.

For Node A, the SSM/I normalized brightness temperature with respect to ground temperature is highly correlated with *SM*. Values of the SSM/I channel transforma-

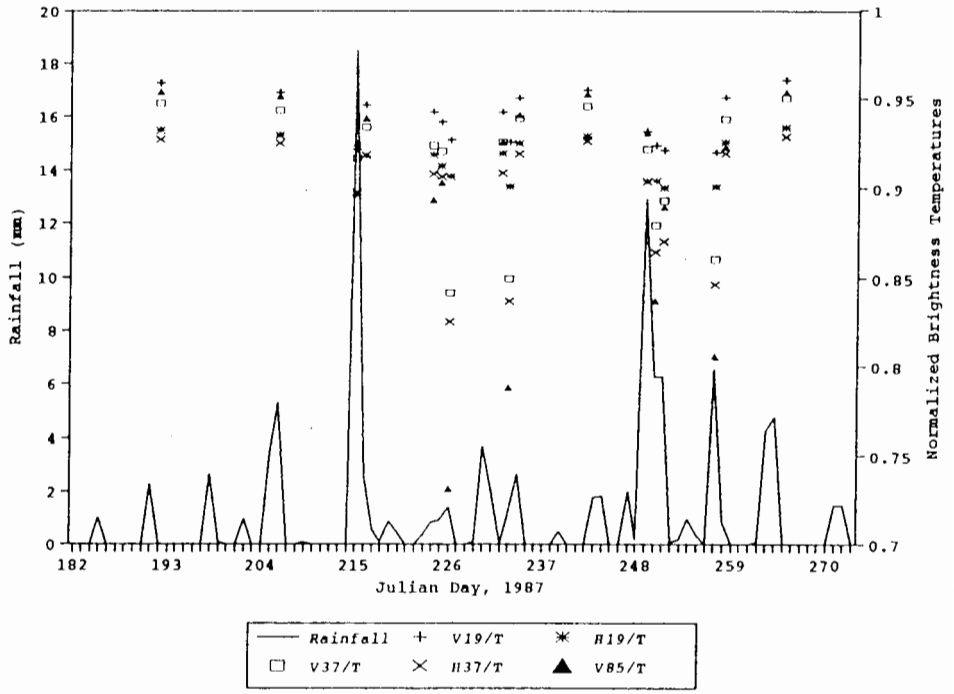

FIG. 4. Time series plots of rainfall and the normalized brightness temperatures for Grid Cell 12 (Node D) between 1 July and 30 September, 1987.

tion without ground temperature are poorly correlated with *SM*. This indicates that the SSM/I brightness temperature variables cannot be used to estimate soil moisture over semi-arid mountainous regions without an estimate of the ground temperature. The best correlation between SSM/I normalized brightness temperature values and soil moisture was obtained between $H37/T$ and soil moisture *SM*. For $SM > 5.0$ mm, the normalized brightness temperature values decrease with increasing the soil moisture.

For Node D, all SSM/I transformation values are poorly correlated with *SM* when all the data are used. When precipitating cloud effects are taken into account, the SSM/I normalized brightness temperature values and some SSM/I transformation amounts become highly correlated with *SM*. The best correlation between SSM/I normalized brightness temperature values and soil moisture was obtained between $H19/T$ and soil moisture *SM*. For $SM > 5.0$ mm, the normalized brightness temperature decreases with increasing soil moisture. Moreover, high correlation coefficients occur between soil moisture *SM* and $H37/V19$ or $V19 - H37$. This indicates that either one of these transformation values of SSM/I brightness temperature can be used to estimate soil moisture over a semi-arid mountainous region without estimating the ground temperature. The linear regression results for the above analysis are summarized in Table 3.

TABLE 3. Results of regression analysis using soil moisture (SM) as dependent variable.

Grid cell	Node	Independent variable	Slope	Intercept	R^2	Number of data
16	A	$H19/T$	- 674.25	633.36	0.64	13
16	A	$H37/T$	- 805.48	754.19	0.80	13
12	D	$H19/T$	- 475.85	443.88	0.79	9
12	D	$V22/T$	- 669.23	637.68	0.74	9
12	D	$H37/V19$	1952.03	- 1884.98	0.68	9
12	D	$H19/H37$	- 1291.72	1302.77	0.63	9
12	D	$V19 - H37$	- 6.76	67.15	0.75	9

For Node A, all data values were used.
For Node D, the data values with $H19\text{-}V85 < 0$ were used.

Test Case

The results of this research indicate the general conditions that are necessary for the SSM/I to infer soil moisture. It is useful to examine the results obtained above; therefore, the results of Grid Cell 12 will be tested. Unfortunately, the number of SSM/I data points is limited. Therefore, the data for Grid Cell 8, which is adjacent to Grid Cell 12, were chosen for this test. Grid Cell 8 (Node D) had 16 data points that will be tested as independent data for the results of Grid Cell 12.

First, the existence of precipitating clouds at the time of the SSM/I overpass will be determined through an examination of the value $H19$ - $V85$. It is found that 8 data points had $H19$ - $V85 > 0$, which are excluded from the analysis. Second, the best single SSM/I channel for a surface soil moisture investigation at satellite descending overpass time will be used. Values of the normalized brightness temperature with respect to ground temperature ($H19/T$) shows that channel 19 is the best one (Table 3). The relevant formula is

$$SM_{H19/T} = 443.88\ [\ 1 - 1.07\ (\ H19/T\ )\ ]$$

where $SM_{H19/T}$ is the soil moisture estimated using normalized brightness temperature of $H19$. The results are shown in Table 4. The soil moisture values obtained from the above formula may have negative values. Because soil moisture cannot be negative, these values can be set equal to zero. The soil moisture values obtained from using normalized brightness temperature values ($H19/T$) have similar patterns to the values SM obtained using ground observation values. It is suggested that the normalized brightness temperatures ($H19/T$) can be used to classify such soil moisture into a quantitatively defined categories.

TABLE 4. Comparison between calculated soil moisture (mm) SM using ground observations and $SM_{H19/T}$ using normalized brightness temperatures ($H19/T$).

SM (mm)	0.1	0.0	0.1	0.0	10.5	0.4	0.0	15.5
$SM_{H19/T}$ (mm)	- 0.7	1.6	- 0.7	1.0	5.3	3.9	0.4	10.9

Conclusion

The main conclusion of the research is that SSM/I channels can be used to classify near-surface soil moisture over a semi-arid mountainous region for the area within the SSM/I footprints (0.25° × 0.25°). For all frequencies, the normalized brightness temperature values were reduced in value after rainfall. Good correlation between soil moisture and normalized brightness temperature was obtained when data on precipitating clouds data at the time of the SSM/I overpass were excluded. A correlation coefficient of – 0.90 was obtained. For the channels of frequency 19.35 and 37.0 GHz, soil moisture affected the horizontal polarization more than it affected the vertical polarization. The normalized brightness temperature in Channel $H19$ with respect to ground temperature ($H19/T$) was the best single SSM/I channel to use for a surface soil moisture investigation at satellite descending overpass time. The normalized brightness temperature in Channel $H37$ with respect to ground temperature ($H37/T$) was the best single SSM/I channel to use for a surface soil moisture investigation at satellite ascending overpass time. Two relationships were found between the near-surface soil moisture and the normalized brightness temperature values. The first relation is that SM is proportional to [$1.00 - 1.07\ (H37/T)$] at Node A, and the second relation is that SM is proportional to [$1.00 - 1.07\ (H19/T)$ at Node D.

Besides soil moisture, other information such as existence of precipitating clouds can be obtained from the brightness temperatures data. The existence of precipitating clouds was determined through an examination of the $V85$ and $H19$ channels. When ($H19 - V85$) is greater than zero, the presence of precipitating clouds at the time of the SSM/I overpass is identified.

The results of this research showed that the developed model, in term of the observed brightness temperature, could be used to classify soil moisture into qualitatively defined categories in the near-surface layers over the southwestern region of Saudi Arabia. Elevation correction for ground temperature is needed to use the SSM/I data to estimate soil moisture in the near-surface layers.

References

Blanchard, B.J., McFarland, M.J., Schmugge, T.J. and **Rhodes, E.** (1981) Estimation of surface soil moisture with API algorithms and microwave emission. *Water Resour. Bull.*, **17,** 767-773.

Burke, W.J. and **Paris, J.F.** (1975) A radiative transfer model for microwave emission from bare agricultural soil. *NASA Tech. Memo. TMX-58166,* NASA Johnson Space Center, Houston, Texas, 27 p.

————, **Schmugge, T.J.** and **Paris, J.F.** (1979) Comparison of 2.8- and 21-cm microwave radiometer observations over soils with emission model calculations. *J. Geophys. Res.*, **84,** 287-294.

Eagleman, J.R. and **Lin, W.C.** (1976) Remote sensing of soil moisture by a 21 cm passive radiometer. *J. Geophys. Res.*, **81,** 3660-3666.

Griffiths, J.R. (1982) *Climate and the Environment.* Westview Press, Inc., Boulder, Colorado.

Linacre, E.T. (1977) A simple formula for estimating evaporation rates in various climates, using temperature data alone. *Agr. Meteorol.*, **18,** 409-424.

McFarland, M.J. (1976) The correlation of Skylab L-Band brightness temperatures with antecedent precipitation. *Preprints Conf. Hydro-Meteorology,* Fort Worth, Texas, 60-65.

————, and **Blanchard, B.J.** (1977) Temporal correlations of antecedent precipitation with Nimbus 5 ESMR brightness temperatures. *Preprints 2nd Conf. Hydrometeor,* Toronto, Ontario, Canada,

Am. Meteor. Soc., 311-315.

————, and **Harder, P.H.** (1982) *Development of an early warning system of crop moisture conditions using passive microwave.* Final Report NAS 9-16556, Remote Sensing Center, Texas A & M University, College Station, Texas, 119 pp.

Newton, R.W. (1977) *Microwave remote sensing and its application to soil moisture detection.* Ph.D. Dissertation, Texas A & M University, College Station, Texas.

————, and **Rouse, J.W.** (1980) Microwave radiometer measurements of soil moisture content. *IEEE Trans., Antennas and Propagation,* AP-**28,** No. 5, 680-686.

————, **Black, Q.R., Makanvand, S., Blanchard, A.J.** and **Jean, B.R.** (1982) Soil moisture information and thermal microwave emission. *IEEE Trans., Geosci. Remote Sensing,* GE-**20,** No. 3, 275-281.

Njoku, E.G. and **Kong, J.** (1977) Theory for passive microwave remote sensing of near-surface soil moisture. *J. Geophys. Res.,* **82,** No. 20, 3108-3118.

————, and **O'Neill, P.E.** (1982) Multifrequency microwave radiometer measurements of soil moisture, *IEEE Trans., Geosci. Remote Sensing,* GE-**20,** No. 3, 468-475.

Poe, G.A. and **Edgerton, A.T.** (1971) *Determination of soil moisture content with airborne microwave radiometry.* Summary report 4006R-2, COM-72-10430, NOAA contract No 1-35378, Hillcrest Heights, Maryland, 43 p.

Schmugge, T.J. (1978) Remote sensing of surface soil moisture. *J. Appl. Meteor.,* **17,** 1549-1557.

———— (1983) Remote sensing of soil moisture: recent advances. *IEEE Trans., Geosci. Remote Sensing,* GE-**21,** No. 3, 336-344.

————, **Jackson, T.J.** and **McKim, H.L.** (1979) *Survey of methods for soil moisture determination.* NASA-TM-80658, Goddard Space Flight Center, Greenbelt, Maryland, 74 p.

————, **Gloersen, G., Wilheit, T.** and **Geiger, F.** (1974) Remote sensing of soil moisture with microwave radiometers. *J. Geophys. Res.,* **79,** 317-323.

Wilheit, T. (1978) Radiative transfer in a plane stratified dielectric. *IEEE Trans., Geosci. Elec.* GE-**16,** 138-143.

Wilke, G.D. (1984) *Multispectral passive microwave correlations with an antecedent precipitation index using the Nimbus 7 SMMR.* M.S. Thesis, Texas A & M University, College Station, Texas.

————, and **McFarland, M.J.** (1986) Correlations between Nimbus-7 scanning multichannel microwave radiometer data and an antecedent precipitation index. *J. Climatol. Appl. Meteorol.,* **25,** 227-238.

تقدير رطوبة التربة السطحية باستخدام الأمواج الدقيقة لتابع فوق المنطقة الجبلية الشبه جافة : دراسة حالة للمنطقة الجنوبية الغربية من المملكة العربية السعودية

عبدالوهاب سليمان مشاط

كلية الأرصاد والبيئة وزراعة المناطق الجافة – جامعة الملك عبدالعزيز – جدة – المملكة العربية السعودية

المستخلص . يهتم هذا البحث بتطبيقات الأمواج الدقيقة السلبية على رطوبة التربة بسبب هطول الأمطار في المنطقة الجنوبية الغربية للملكة العربية السعودية . تمت دراسة حالتين للتحقق من تجارب حرارات السطوع لرطوبة التربة . الحالة الأولى عند صعود التابع (حوالي السادسة صباحًا) والثانية عند انحدار التابع (حوالي الساعة السادسة مساءً) .

من خلال الحالتين وجد أن حرارة السطوع المعيارية بالنسبة لدرجة حرارة سطح الأرض يمكن أن تدل عن رطوبة التربة السطحية . كذلك وجد أن حرارة السطوع المعيارية ليست حساسة لرطوبة التربة عند وجود سحب ممطرة والتي يمكن معرفة وجودها من خلال فحص حرارة السطوع ذات تردد ٨٥,٥ قيقاهرتز .